Security of Infocommunication Systems and Internet of Things

2025 Vol 3, No 1

https://doi.org/10.31861/sisiot2025.1.01012

Received 09 June 2025; revised 29 June 2025; accepted 30 June 2025; published 30 June 2025

Telecommunication System for Transmission of Adaptively Scaled Digital Images

Yurii Hnatiuk*

Radio Engineering and Information Security Department, Yuriy Fedkovych Chernivtsi National University, Chernivtsi, Ukraine

*Corresponding author (E-mail: hnatiuk.yurii@chnu.edu.ua)

ABSTRACT The hardware and software of a telecommunication system designed for the transmission of adaptively scaled digital images has been developed. The system consists of transmission and reception subsystems. The hardware of the transmission subsystem includes a USB video camera, a microcomputer Raspberry Pi3 and a Raspberry Pi3 radio module. The hardware of the reception subsystem includes a radio module nRF24L01 # 2, a microcontroller Funduino Uno and a computer. The radio module Funduino Uno has a relatively low transmission speed, but provides low power consumption. The system software has been developed in Python and C++. In the transmission subsystem, the image from the video camera is read using the program cam2nrf, its scale is reduced by interpolation and the reduced image is transmitted via radio module # 1. In the reception subsystem, the reduced image is read via radio module # 2, its scale is increased by interpolation. Image scaling is performed using bilinear or bicubic interpolation. The program nrf_rx, which runs on the Funduino Uno microcontroller, is used to receive wireless data using the radio module nRF24L01. The program recv_img, which runs on the computer, reads the image from the microcontroller Funduino Uno, scales, visualizes and saves it. Scaling adaptability is ensured by choosing the image interpolation algorithm depending on its average spatial period TCR, which is calculated based on the Fourier power spectrum of the original image. For values TCR < 4.5 pixels, bilinear interpolation is performed, and otherwise bicubic interpolation is performed. Testing of the telecommunication system for transmitting real images shows its operability. By reducing the image size by a factor of 2, the transmission time is reduced by a factor of 4 with a slight decrease in the visual quality of the resulting image. Such image scaling is especially effective when transmitting images over low-bandwidth channels. The developed hardware and software can be used in `Internet of Things systems for image transmission.

KEYWORDS telecommunication systems, digital image scaling, interpolation algorithms, video camera, Internet of Things.

I. INTRODUCTION

Modern telecommunication systems are often used to transmit both individual images and frames of a video stream. Image transmission is important, in particular, in video surveillance and remote control systems [1-3]. In the case of using low-bandwidth communication channels, an effective way to reduce traffic in the system is to transmit images at a reduced scale [1, 4]. In such telecommunication systems, on the transmitting side, the original *fRGB* color images are read from video cameras and scaled to smaller *fRGBs* images, which are transmitted over telecommunication channels.

On the receiving side, *fRGBs* images are read and scaled to *fRGBs*2 images, the size of which is equal to the size of *fRGB*. Bilinear and bicubic interpolation algorithms [5, 6] are often used for image scaling, which have low computational complexity and high performance, compared to nonlinear interpolation algorithms [7, 8] and artificial neural networks (ANN) [9-14]. In addition, image scaling using ANN is characterized by quite high visual quality, but also a high probability of artifacts.

The problem is that image interpolation algorithms have relatively low accuracy. This leads to the appearance of characteristic defects in images, in particular, blurring of contours and loss of detail [15, 16]. Analysis of the results of image scaling shows that scaling errors depend not only on the interpolation algorithm, but also on the spatial distribution of image brightness. Therefore, the goal of this work is relevant, which is to develop a telecommunication system for transmitting adaptively scaled digital images. Scaling adaptability is ensured by choosing an interpolation algorithm depending on the spatial distribution of image brightness, which is described by its average spatial period.

II. STRUCTURE AND HARDWARE OF THE TELECOMMUNICATIONS SYSTEM

The structure of the developed telecommunication system is described by a diagram (Fig. 1), which consists of transmission and reception subsystems. The initial images of the studied objects are read using a USB video camera [17] connected to a Raspberry Pi3 microcomputer. Reading of *fRGB* color images from the video camera is performed by the program cam2nrf in Python, which also performs scaling of *fRGB* images into smaller *fRGBs* images (with a scaling factor S_{c1}, for example $S_{c1} = 0.5$).

Digital color images are processed programmatically as arrays fRGB(i, k, c), where $i = 0,..., M-1$; $k = 0,..., N-1$; $c = 0,..., Q_C-1$; M is the image size in height (in pixels), N is the image size in width, $Q_C = 3$ is the number of color channels (RGB) [2]. The image scale is reduced by the interpolation algorithm. After that, the *fRGBs* images are transmitted via telecommunication channels by the program cam2nrf. For remote signal transmission, radio modules nRF24L01 # 1 and # 2 were used on the transmitting and receiving sides, respectively (Fig. 2).

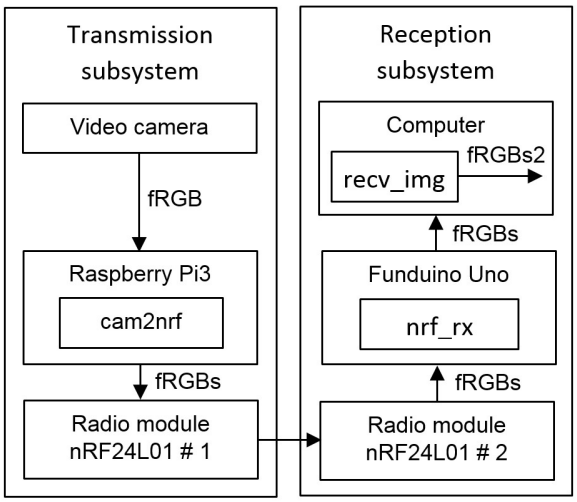

FIG. 1. Structural diagram of a telecommunications system.

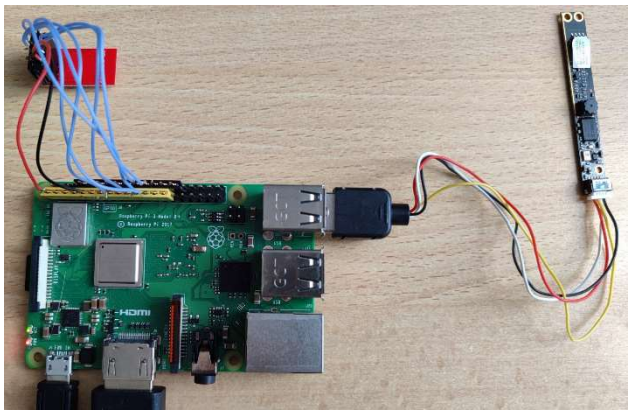

FIG. 2. Implementation of the transmission subsystem: video camera (right), Raspberry Pi3 microcomputer and nRF24L01 radio module # 1 (top left).

On the receiving side, the *fRGBs* images are read from radio module #2 using the microcontroller Funduino Uno (Fig. 3) under the control of the program nrf_rx (in C++). The Funduino Uno is physically connected to the computer via a USB port, but the image is transferred from the device to the computer via a virtual serial port in software.

The *fRGBs* images are read in the computer by the recv_img program (in Python), which also scales the *fRGBs* images to *fRGBs*2 images (scale factor S_{c2}, e.g. $S_{c2} = 2$).

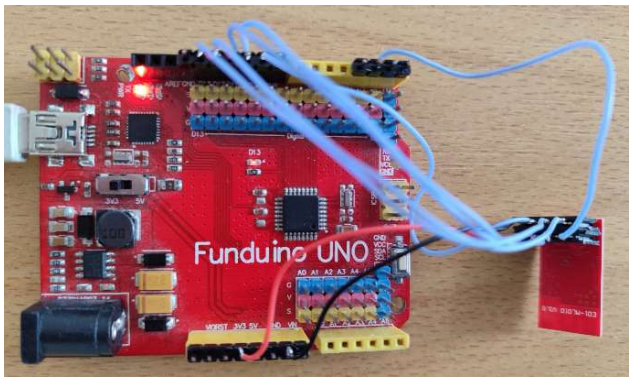

FIG. 3. Implementation of the reception subsystem: nRF24L01 radio module # 2 (right), Funduino Uno microcontroller.

The nRF24L01 radio module operates at a frequency of 2.4 GHz and supports data transfer rates of up to 2 Mbps in transmitter or receiver mode (at a distance of up to 520 m). At a distance of up to 1000 m, the transmission rate via the radio module is 250 Kbit/s. The radio module is controlled using the SPI protocol and consumes a small current (up to 115 mA) at a supply voltage of 3.6 V. When transmitted via the radio module, data is divided into packets of 32 bytes.

III. TELECOMMUNICATIONS SYSTEM SOFTWARE

In the cam2nrf program (transmission subsystem), reading images as frames of a video stream from a USB video camera is performed using the OpenCV library. By default, the program saves images in JPEG format (for data compression purposes). The degree of image compression depends on their resolution, noise level [18], requirements for visual image quality, and other factors. The nRF24L01 wireless radio module # 1 is controlled using the RF24 software module. Reading, processing, and transmitting images in the cam2nrf program is divided into the following stages:

1. Reading the image from the video camera.
2. Reducing the image size.
3. Converting the image to JPEG format.
4. Sending the image via the nRF24L01 radio module (first the file size is sent, and then in the loop the image fragments are sent as 32-byte packets).

The nrf_rx program, which runs on the Funduino Uno microcontroller, is used to receive wireless data using the nRF24L01 #2 radio module, setting it to receiver mode. The nrf_rx program waits for radio signals to be received and displays the received data in the Serial Monitor. The radio signal power can be set in the range from RF24_PA_MIN to RF24_PA_MAX, where the RF24_PA_LOW value provides minimal power consumption. The transmission speeds are set from the following list: 250kbps, 1Mbps, 2Mbps.

In the recv_img program (reception subsystem), which is executed on the computer, reading an image from the Funduino Uno microcontroller is divided into the following stages:

1. Waiting for a header with the image size.
2. Reading image packets.
3. Decoding the received packets into an image.
4. Zooming the image (for example, 2 times).
5. Visualizing and saving the image.

Ideally, the original *fRGB* (Fig. 4) and the scaled *fRGBs*2 image should match. However, due to scaling, differences are observed between the images. The scaling error was calculated from the difference between the *fRGB* and *fRGBs*2 images as the root mean square error (*RMSE*) according to the equation:

$$R_{MSE} = \sqrt{\frac{1}{M \cdot N \cdot Q_C} \sum_{i=0}^{M-1} \sum_{k=0}^{N-1} \sum_{c=0}^{Q_C-1} \left[\Delta_{fRGB}\right]^2}, \quad (1)$$

where $\Delta fRGB = fRGB(i, k, c) - fRGBs2(i, k, c)$; $i = 0,..., M-1$; $k = 0,..., N-1$; $c = 0,..., Q_C-1$; M is the image size in height; N is the image size in width; $Q_C = 3$ is the number of color channels.

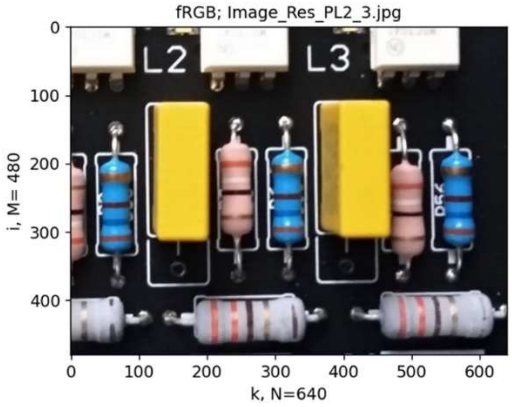

FIG. 4. Initial fRGB image.

The choice of interpolation algorithm (bilinear or bicubic) when changing the image scale is the scaling error RMSE (1) and is performed taking into account its average spatial period *TCR*, which is calculated based on the Fourier power spectrum *PS* [19, 20] of the image *fn*, which is obtained from the initial *fRGB*. A square grayscale image *fn* with dimensions *Md* × *Nd* pixels is used, where *Md* = *Nd* = min(*M*, *N*). The power spectrum *PS* (Fig. 5) is calculated as the square of the modulus of the centered Fourier spectrum of the image *fn*. The power spectrum is calculated as an array *PS*(*m, n*), where *m* is the number (index) of the spatial frequency in height, *n* is the frequency number in width, *m* = 0, 1, ..., *Md*-1; *n* = 0, 1, ..., *Nd*-1.

Based on the power spectrum *PS*, its averaged radial profile *PR* (*d*) is calculated, where *d* = 0, 1, ..., *NR*-1, where *NR* = [*Md*/2]+1 (Fig. 6). The radial profile *PR*(*d*) describes the dependence of the amplitudes of the *PS* spectrum (averaged over all directions) on the frequency numbers *d*. The frequency numbers *d* are defined as integer values of the distances from the elements of the *PS* spectrum to its center.

The value of *PR*(*d*) is calculated as the arithmetic mean of the coefficients of the power spectrum *PS*(*m, n*), for which the distance to the center of the spectrum is equal to *d*. The radial spatial frequency *vr* is calculated through its number *d* by the formula:

$$v_r = \frac{d}{2(N_R - 1)}. \qquad (2)$$

The average spatial frequency *vCR* of the image is calculated based on a given interval ($[NR \cdot 0.25] \le d \le NR$) for the radial profile *PR*(*d*) as its center of gravity. The average spatial period *TCR* of the image is calculated by the formula:

$$T_{CR} = \frac{1}{v_{CR}}. \qquad (3)$$

The *TCR* period is calculated by the cam2nrf program after reading the image from the video camera and transmitted to the receiving side.

By studying a series of images [21, 22], it was found that for values of the period *TCR* < 4.5 pixels, a smaller interpolation error is provided by bilinear interpolation, and otherwise by bicubic interpolation.

For a series of images of the same type, the *TCR* period can be calculated only once.

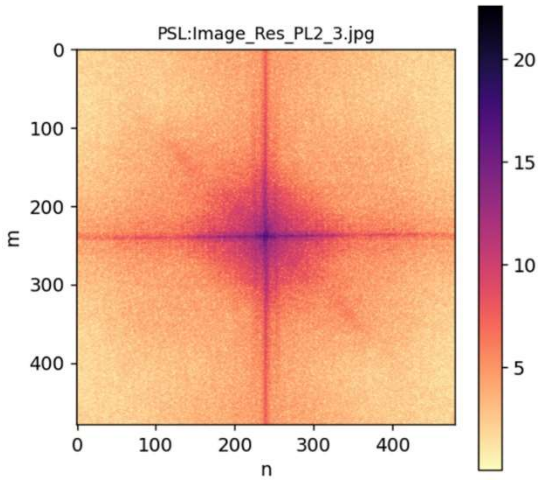

FIG. 5. Fourier power spectrum PS image fn (in logarithmic scale).

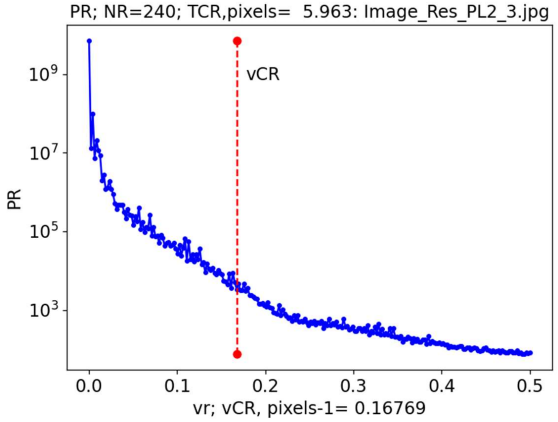

FIG. 6. Radial profile PR for the power spectrum.

IV. TELECOMMUNICATIONS SYSTEM TESTING

A telecommunication system for transmitting adaptively scaled digital images was tested using the example of reading the initial *fRGB* image (Fig. 4). Based on the initial image, a reduced-scale *fRGBs* image was calculated (Fig. 7a). The *fRGBs* image was sent via the radio channel of the telecommunication system, after which it was converted into an enlarged *fRGBs*2 image on the receiving side (Fig. 7b).

For the studied image, the average spatial period *TCR* = 5.96 > 4.5 pixels, therefore, the bicubic interpolation algorithm was chosen. The root mean square scaling error *RMSE* (1) for bicubic interpolation is 0.0187, which is significantly less than RMSE = 0.0279 for bilinear interpolation. The higher accuracy of bicubic interpolation for this case is illustrated by the profiles of the original *fRGB* and scaled *fRGBs*2 images (Fig. 8). In the case of bicubic interpolation, the profile of the scaled image differs less from the profile of the original.

At a transmission rate of 1 Mbit/s, the transmission time of an image of 640 × 480 pixels is 12 s. By reducing the image size by a factor of 2 (when transmitting in a telecommunication system), the transmission time is reduced by a factor of 4. The results of the research showed that the image after reduction and enlargement of the scale is restored with satisfactory quality, i.e. the developed telecommunication system is operational.

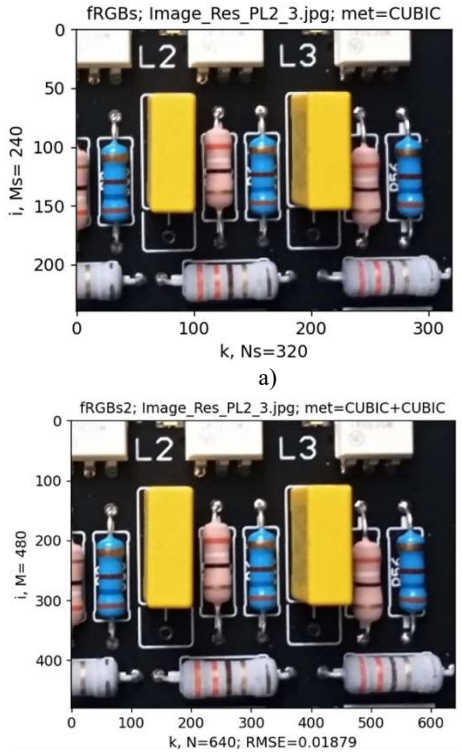

FIG. 7. Down-scale fRGBs image (a) and up-scale fRGBs2 image (b).

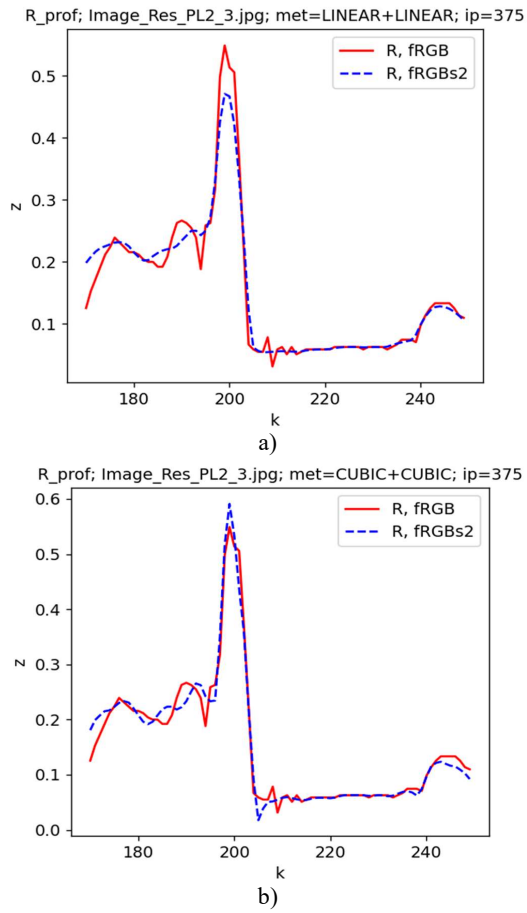

FIG. 8. Profiles z(k) for the red color channel of the original image fRGB and the scaled image fRGBs2: (a) scaling is performed using the bilinear interpolation algorithm; (b) scaling is performed using the bicubic interpolation algorithm; ip is the number of the image pixel row.

V. CONCLUSION

The hardware and software of the telecommunication system for transmitting adaptively scaled digital images has been developed. The hardware of the system includes a video camera, a Raspberry Pi3 microcomputer and nRF24L01 radio modules # 1 and # 2, a Funduino Uno microcontroller and a computer. The system software is developed in Python and C++.

The image scaling was performed using bilinear or bicubic interpolation algorithms. Scaling adaptability was implemented by selecting the image interpolation algorithm depending on its average spatial period. It was found that for period values $TCR < 4.5$ pixels, bilinear interpolation provides a smaller interpolation error, and in other cases, bicubic interpolation.

By reducing the image size during transmission by 2 times, the transmission time was reduced by 4 times, while the visual quality of the resulting image decreased slightly.

The developed hardware and software can be used to transmit images between Internet of Things devices in wireless systems, for example, in smart robots, drones, or in video surveillance systems.

AUTHOR CONTRIBUTIONS

Yu.H – conceptualization, methodology, software, resources, writing-original draft preparation, writing-review and editing, visualization, validation, investigation.

COMPETING INTERESTS

The author declares no conflict of interest.

REFERENCES

[1] R. Gonzalez and R. Woods, *Digital Image Processing*, 4th ed. New York, NY, USA: Pearson/Prentice Hall, 2018.

[2] S. V. Balovsyak, O. V. Derevyanchuk, Ya. V. Derevianchuk, V. V. Tomash, and S. V. Yarema, "Segmentation of railway transport images using fuzzy logic," *Trans Motauto World*, vol. 7, no. 3, pp. 122–125, 2022.

[3] Zh. Hu, D. Uhryn, Yu. Ushenko, V. Korolenko, V. Lytvyn, and V. Vysotska, "System programming of a disease identification model based on medical images," in *Proc. SPIE: Sixteenth Int. Conf. Correlation Optics*, vol. 12938, pp. 129380F-1–129380F-4, 2024. doi: 10.1117/12.3009245.

[4] S. Palani, *Principles of Digital Signal Processing*. Cham, Switzerland: Springer, 2022.

[5] D. Kim and D. Hwang, Eds., *Intelligent Imaging and Analysis*. Basel, Switzerland: MDPI, 2020.

[6] W. Burger and M. J. Burge, "Geometric Operations," in *Digital Image Processing. Texts in Computer Science*. Cham, Switzerland: Springer, 2022, pp. 601–637. doi: 10.1007/978-3-031-05744-1_21.

[7] G. Liu, "The novel bilateral quadratic interpolation image super-resolution algorithm," *Int. J. Image, Graphics and Signal Process.* (IJIGSP), vol. 13, no. 3, pp. 55–61, 2021. doi: 10.5815/ijigsp.2021.03.05.

[8] P. Prystavka and O. Cholyshkina, "Pyramid image and resize based on spline model," *Int. J. Image, Graphics and Signal Process.* (IJIGSP), vol. 14, no. 1, pp. 1–14, 2022. doi: 10.5815/ijigsp.2022.01.01.

[9] S. Balovsyak, I. Fodchuk, Kh. Odaiska, Yu. Roman, and E. Zaitseva, "Analysis of X-ray Moiré images using artificial neural networks," in *Proc. 3rd Int. Workshop Intelligent Inf. Technol. Syst. Inf. Security (IntelITSIS)*, Khmelnytskyi, Ukraine, Mar. 23–25, 2022, CEUR Workshop Proc., pp. 187–197.

[10] Waifu2x. [Online]. Available:

https://waifu2x.udp.jp/index.uk.html
[11] A. Geron, *Hands-On Machine Learning with Scikit-Learn, Keras, and TensorFlow*. Sebastopol, CA, USA: O'Reilly Media, 2019.
[12] O. Berezsky, P. Liashchynskyi, O. Pitsun, P. Liashchynskyi, and M. Berezkyy, "Comparison of deep neural network learning algorithms for biomedical image processing," *CEUR Workshop Proc.*, pp. 135–145, 2022.
[13] K. Mahmut, "Image interpolation with spiking neural network based pixel similarity," *Signal, Image and Video Process.*, vol. 18, pp. 6925–6936, 2024. doi: 10.1007/s11760-024-03362-3.
[14] Z. Cheng, "Research on image up-scaling and super-resolution based on convolutional neural network," *Highlights Sci., Eng. Technol.*, vol. 72, pp. 1258–1263, 2023. doi: 10.54097/ef4k8k08.
[15] D. Suresha and H. N. Prakash, "Data content weighing for subjective versus objective picture quality assessment of natural pictures," *Int. J. Image, Graphics and Signal Process.* (IJIGSP), vol. 9, no. 2, pp. 27–36, 2017.
[16] S. Balovsyak and Y. Hnatiuk, "Analysis of results of scaling digital images by interpolation algorithms," *Security Infocommun. Syst. Internet Things (SISIOT)*, vol. 2, no. 1, pp. 1–6, 2024. doi: 10.31861/sisiot2024.1.01007.
[17] S. Balovsyak, Kh. Odaiska, O. Yakovenko, and I. Iakovlieva, "Adjusting the brightness and contrast parameters of digital video cameras using artificial neural networks," in *Proc. SPIE: Sixteenth Int. Conf. Correlation Optics*, vol. 12938, pp. 129380I-1–129380I-4, 2024. doi: 10.1117/12.3009429.
[18] S. V. Balovsyak and Kh. S. Odaiska, "Automatic highly accurate estimation of Gaussian noise level in digital images using filtration and edges detection methods," *Int. J. Image, Graphics and Signal Process.* (IJIGSP), vol. 9, no. 12, pp. 1–11, 2017. doi: 10.5815/ijigsp.2017.12.01.
[19] S. Sharma and T. Varma, "Discrete combined fractional Fourier transform and its application to image enhancement," *Multimedia Tools Appl.*, vol. 83, pp. 29881–29896, 2024. doi: 10.1007/s11042-023-16742-7.
[20] E. Rajaby and S. M. Sayedi, "A structured review of sparse fast Fourier transform algorithms," *Digit. Signal Process.*, vol. 123, 103403, 2022. doi: 10.1016/j.dsp.2022.103403.
[21] C. Fowlkes, D. Martin, and J. Malik, "Local figure/ground cues are valid for natural images," *J. Vision*, vol. 7, no. 8, pp. 1–9, 2007.
[22] The Berkeley Segmentation Dataset and Benchmark. BSDS300. [Online]. Available: https://www.eecs.berkeley.edu/Research/Projects/CS/vision/bsds

Yurii Hnatiuk

In 2019, graduated from Chernivtsi National University with a degree in "Computer Engineering". In 2002, entered postgraduate studies in the specialty "Telecommunications and radio engineering". Research interests include digital signal and image processing, programming, artificial neural networks.

ORCID ID: 0009-0006-5605-9281

Телекомунікаційна система для передавання адаптивно масштабованих цифрових зображень

Юрій Гнатюк*

Кафедра радіотехніки та інформаційної безпеки, Чернівецький національний університет імені Юрія Федьковича, Чернівці, Україна
*Автор-кореспондент (Електронна адреса: hnatiuk.yurii@chnu.edu.ua)

АНОТАЦІЯ Розроблено апаратно-програмне забезпечення телекомунікаційної системи, яка призначена для передавання адаптивно масштабованих цифрових зображень. Система складається з підсистем передачі та прийому. Апаратне забезпечення підсистеми передачі містить USB-відеокамеру, мікрокомп'ютер Raspberry Pi3 та радіомодуль nRF24L01 №1. Апаратне забезпечення підсистеми прийому містить радіомодуль nRF24L01 №2, мікроконтролер Funduino Uno та комп'ютер. Радіомодуль nRF24L01 має відносно низьку швидкість передачі, але забезпечує низьке енергоспоживання. Розроблено програмне забезпечення системи на мові Python та C++. У підсистемі передачі за допомогою програми cam2nrf зчитується зображення з відеокамери, зменшується його масштаб методом інтерполяції і виконується передача зменшеного зображення через радіомодуль №1. У підсистемі прийому зчитується зменшене зображення через радіомодуль №2, збільшується його масштаб методом інтерполяції. Зміна масштабу зображень виконується методом білінійної або бікубічної інтерполяції. Програма nrf_rx, яка виконується на мікроконтролері Funduino Uno, використовується для прийому бездротових даних за допомогою радіомодуля nRF24L01. У програмі recv_img, яка виконується на комп'ютері, виконується зчитування зображення з мікроконтролера Funduino Uno, його масштабування, візуалізація та збереження. Адаптивність масштабування забезпечується за рахунок вибору алгоритму інтерполяції зображення залежно від його середнього просторового періоду TCR, який обчислюється на основі енергетичного спектру Фур'є початкового зображення. Для значень періоду TCR < 4.5 пікселів виконується білінійна інтерполяція, а в іншому випадку – бікубічна. Тестування телекомунікаційної системи для передаванні реальних зображень показано її працездатність. За рахунок зменшення розміру зображення у 2 рази час передачі зменшується у 4 рази при незначному зниженні візуальної якості зображення-результату. Таке масштабування зображень особливо ефективне при передачі зображень через канали з низькою пропускною здатністю. Розроблене апаратно-програмне забезпечення може використовуватися в системах Інтернету речей для передачі зображень.

КЛЮЧОВІ СЛОВА телекомунікаційні системи, масштабування цифрових зображень, алгоритми інтерполяції, відеокамера, Інтернет речей.